Abstract

Small artificial waterbodies are larger emitters of carbon dioxide (CO2) and methane (CH4) than natural waterbodies. The Intergovernmental Panel on Climate Change (IPCC) recommends these waterbodies are accounted for in national emission inventories, yet data is extremely limited for irrigated landscapes. To derive a baseline of their greenhouse gas (GHG) footprint, we investigated 38 irrigation farm dams in horticulture and broadacre cropping in semi-arid NSW, Australia. Dissolved CO2, CH4, and nitrous oxide (N2O) were measured in spring and summer, 2021-2022. While all dams were sources of CH4 to the atmosphere, 52% of irrigation farm dams were sinks for CO2 and 70% were sinks for N2O. Relationships in the linear mixed effect models indicate that CO2 concentrations were primarily driven by dissolved oxygen (DO), ammonium, and sediment carbon content, while N2O concentration was best explained by an interaction between DO and ammonium. Methane concentrations did not display any relationship with typical biological variables and instead were related to soil salinity, trophic status, and size. Carbon dioxide-equivalent emissions were highest in small (<0.001 km2) dams (305 g CO2-eq m-2 season-1) and in those used for recycling irrigation water (249 g CO2-eq m-2 season-1), with CH4 contributing 70% of average CO2-eq emissions. However, irrigation dams had considerably lower CH4 emissions (mean 40 kg ha-1 yr-1) than the IPCC emission factor (EF) of 183 kg CH4 ha-1 yr-1 for constructed ponds and lower N2O EF of 0.06% than the indirect EF for agricultural surface waters (0.26%). This synoptic survey reveals existing models may be severely overestimating (4-5 times) farm dam CH4 and N2O emissions in semi-arid irrigation areas. Further research is needed to define these artificial waterbodies in emissions accounting.

INTRODUCTION

Artificial agricultural ponds are increasingly recognised as sources of greenhouse gas emissions (GHGs), and are often reported as higher emitters of methane (CH_4) than natural freshwaters (Ollivier et al. 2019a; Peacock et al. 2021). Research efforts have recently focused on the contribution of farm dams, a type of agricultural pond, to anthropogenic emissions of CH_4, carbon dioxide (CO_2), and nitrous oxide (N_2O) (Ollivier et al., 2019a; Malerba et al. 2022a). These human-made waterbodies store water on-farm for crop or livestock production and include newly created “ponds” or small impoundments of a natural waterway, and will henceforth be referred to as farm dams. Artificial ponds in Queensland, Australia, are estimated to contribute 10% of the state’s total emissions from land use, land use change and forestry. Additional studies show that farm dams can contribute three times more CO_2-equivalent emissions than reservoirs (Ollivier et al. 2019a) and that nutrients from manure inputs are a significant driver (Malerba et al. 2022b). Complementary studies of semi-arid farm dams in the Northern hemisphere have shown similar patterns between nutrient enrichment and CH_4 emissions, but despite high nutrient levels, N_2O is often consumed within these systems (Jensen et al. 2023; Webb et al. 2019a; Webb et al. 2019b). With growing attention is being paid to accounting that has previously overlooked sources of GHGs (CO_2, CH_4, N_2O), such as those from aquatic ecosystems (Lindroth and Tranvik, 2021) the contribution of artificial ponds to GHG budgets in irrigated agriculture remains a major knowledge gap (hereafter, referred to as "irrigation farm dams").

Irrigated agriculture is a common practice in arid and semi-arid regions where precipitation is not enough to meet crop water requirements. Globally, irrigated agriculture makes up 3.6 million km^2 and has had direct impacts on landscapes, including intensifying the surface energy balance, increased uptake of carbon and nitrogen in crops, and enhance to soil nitrogen mobilisation (McDermid et al. 2023). High-density artificial waterbodies, such as farm dams for water storage and channels for water conveyance and drainage, have been created for irrigated crop production. Collectively, these artificial waterbodies represent a sophisticated network of water supply and reticulation that is critical for sustaining agricultural productivity and social-economic sustainability in dryland environments. On the farm, irrigation farm dams, commonly known in Australia as "water storages" (Craig et al. 2005) or in other countries as "irrigation ponds" (Aguilera et al. 2019), can be used for purposes such as permanent or temporary irrigation water storage, rainwater storage, recycling irrigation water between fields, settling sediments for drip irrigation, and household irrigation. Depending on their primary function, irrigation type (e.g. drip, surface furrow) and size, irrigation farm dams can be broadly classified as settling ponds, storages, recycle dams, and turkey nests (Table S1).

Unlike dams used in other agricultural practices, irrigation farm dams are built to meet the dynamic requirements of irrigated farming systems. Therefore, the biogeochemical functioning and subsequent potential for GHG production will likely be intensified in irrigation farm dams compared to dams in non-irrigated agriculture. Irrigation farm dams often have high nutrients, receive crop residue inputs rather than animal manure, and exist in climate zones with high sunlight exposure and hot conditions. However, a lack of empirical data from field studies has hindered accurate representation of irrigation waterbodies in GHG assessments. For example, irrigation waterbodies have the most limited N_2O dataset out of other agricultural surface waters that make up the default N_2O emissions factors for nitrogen leaching and runoff (EF_5, Webb et al. 2021) and represent just 14% of the CH_4 emission factor (EF) dataset for "*Other Constructed Waterbodies*" (IPCC, 2019). In the only known reported carbon footprint study of the irrigation sector (Aguilera et al. 2019), irrigation farm dams were assigned the global average CH_4 EF for reservoirs as no data specific to irrigation waterbodies was available.

Comprehensive field studies are required to develop a baseline of GHG emissions from irrigation dams to provide a basis for methodological refinement of EFs used in national inventory reporting. The United States and Australia have included farm dam CH_4 emissions in their latest National Greenhouse Gas Inventory reports submitted to the United Nations Framework Convention on Climate Change (UNFCCC, 2021). A meta-analysis of farm dam CH_4 emissions revealed that the contribution of small (<8 ha) on-farm waterbodies is likely underestimated in these reports (Malerba et al. 2022a), however, semi-arid irrigation farm dams were not represented in the global dataset. As a first step to addressing the data gap, we aimed to quantify CO_2, CH_4, and N_2O emissions from irrigation farm dams covering a broad range of semi-arid agricultural systems in eastern Australia. Specific objectives were to: 1) establish baseline GHG emissions from farm dams across diverse irrigated summer crops including perennial horticultural land uses; 2) determine the environmental drivers of CO_2, CH_4, and N_2O; and 3) calculate regional farm dam emissions to compare with IPCC emission factors for agricultural waterbodies.

METHODS

Two spatial surveys of irrigation farm dams were carried out to capture variability in water conditions between spring and summer 2021-2022. Farm dam sites were located in the Murrumbidgee Irrigation Area (MIA) and the Coleambally Irrigation Area (CIA) which are part of the Murrumbidgee River catchment within the greater Murray Darling Basin, Australia (Figure S1). Together, these irrigation areas represent the third largest irrigation area (~7,800 km^2) in Australia and support a diverse production of food and fibre including broadacre cotton, rice, wine grapes, citrus, and almonds. The climate is semi-arid with hot summers (mean maximum temperature 31.3°C) and cool winters (mean maximum 17.6°C) and a mean annual rainfall of 404 mm (Australian Bureau of Meteorology, 2023).

Farm dam surface water area was calculated from the most recent satellite imagery on Google Earth (Google, California, United States) using the polygon tool. Waterbodies range from 180-145,000 m^2 in surface area. Because some recycle farm dams are drained during field irrigation, it was not possible to sample five recycle dams in summer. Four classifications of irrigation dam types were identified based on farmer definitions and visual inspections: settling ponds n = 5; storage dams; n = 8; recycle dams n = 19; and turkey nests n = 6 (see Table S1 for definitions).

Field measurements

Surface water GHG concentrations, water quality, sediments and surrounding soil were sampled from 38 farm dams between September 2021 and April 2022 (Figure S1). All water samples and measurements were taken 1-2 m from the dam margin at 0.3 m under the water between 10:00 and 14:00. Water quality variables were measured on site using a portable multiparameter meter (HI98194, Hanna Instruments) and included temperature, pH, dissolved oxygen (DO), electrical conductivity (EC), and atmospheric pressure. Barometric atmosphere pressure was also recorded using the Hanna Instruments multiparameter meter. Phosphate concentrations were measured on site using a portable Phosphate colorimeter (HI713, Hanna Instruments). Water samples were collected into two 60 mL polypropylene bottles and transported on ice back to the laboratory for nitrate (NO_3^-) and ammonium (NH_4^+) analysis. Samples were analysed the same day using a Hach HQ440d benchtop meter (Hach Company, Colorado, United States) equipped with a NO_3^- and NH_4^+ ion-selective electrode (detection limit 0.1 mg/L NO_3-N, 0.018 mg/L NH_4-N), or frozen for subsequent analysis the following day. Samples were brought to room temperature prior to measurement.

Three sediment samples were collected 1-2 m from the dam margin in the water using polycarbonate coring tubes by pushing the core into the sediment until a hard clay layer was reached. The top 10 cm from each core was sectioned off in the field and the three replicates bagged into one sample for each site. Sediments were stored in plastic Ziplock bags at 4°C until the completion of each survey. Samples were dried at 60°C until constant mass was reached (~ 4 days) and the dry weight recorded to calculate the approximate dry bulk density (DBD, g dry mass cm^{-3}) using the total volume of the three cores (435 cm^3). Composite sediment samples were ground to pass through a 2-mm sieve prior to laboratory analysis. Samples were analysed for total %C, %N on a LECO CNS928 Series Macro Determinator (LECO Corporation, St. Joseph, Michigan, United States) and $\delta^{13}C$, and $\delta^{15}N$ on a Sercon 20-22 continuous-flow isotope ratio mass spectrometer (Sercon Ltd, Cheshire, UK). C to N ratio (C/N) was calculated from the C and N content. Total C stock to 10 cm of each sampled waterbody was determined by multiplying %C by DBD and upscaled to each dam area.

Soil surface pH and EC were measured on site in soils bordering (within 10 m from dam wall) the farm dam to test if soil properties influence water emissions. A portable soil pH meter (HI99121, Hanna Instruments) and direct soil EC tester (HI98331, Hanna Instruments) were used to take three spot measurements from around the dam. A 0.3 m hole was dug prior to inserting the probes into the soil to take readings. If the substrate was dry, deionised water was added until the substrate was saturated to get a reading.

Greenhouse gas measurements

Two dissolved GHG samples were taken at each farm dam using the headspace equilibration method (Hope et al. 2004). While in the field, 25 mL of "Zero air" (Coregas Ltd, Griffith, NSW, Australia) was withdrawn from a 1-L Tedlar® film bag (DuPont de Nemours, Inc, Delaware, United States) using a 100-mL syringe and shaken together with 75 mL of sample water for 2 minutes. The headspace air was transferred into two pre-evacuated 12 mL soda glass vials fitted with a double wadded cap. Samples were stored at room temperature for a maximum of one month before being sent for laboratory analysis. Headspace concentrations for GHGs were measured using gas chromatography (GC) with an Agilent 7890A GC (Agilent Technologies, Inc., Santa Clara, CA, United States) and calculated using standard curves. The dry molar fractions of CO_2, CH_4, and N_2O were corrected for dilution and converted to dissolved concentrations according to solubility coefficients (Weiss 1974; Weiss & Price 1980; Yamamoto et al. 1976), considering the water temperature, salinity, and barometric pressure at each site. At 10 sites in spring, headspace CO_2 concentrations were not determined as they were below the detection level of the GC (<50 ppm) due to high pH in these waterbodies (~9.16). For these sites, we gap filled the CO_2 data with the relationship between dissolved CO_2 levels and surface water pH values for dams in the spring survey (Figure S2).

To estimate GHG emissions from irrigation dams, we calculated diffusive fluxes using dissolved gas concentrations (C_{water}) and dam-specific gas transfer velocity (k_{600}) values in the following equation:

$$F = k_{600}(C_{water} - C_{air})$$

where F is the flux (mmol m^{-2} d^{-1}) of CO_2, CH_4, or N_2O (μmol m^{-2} d^{-1}) across the water-air interface, k_{600} (m d^{-1}) is normalised to a Schmidt number of 600, and C_{air} is the dissolved gas concentrations at atmospheric equilibrium where 416, 1.91, and 0.335 ppm were used for CO_2, CH_4, and N_2O, respectively (Mauna Loa NOAA station, September 2021–March 2022). Farm-dam specific gas transfer velocity values of 0.78 (CO_2), 0.48 (CH_4), and 0.76 (N_2O) were applied to flux calculations using the mean k_{600} determined in 50 individual floating-chamber measurements taken on a subset of sites (n = 17) during a pilot study in April 2021 (Table S3).

Analysis

All statistical analysis was performed in R for Windows (version 4.2.2; R Core Team, 2022) and plotted using the "ggplot2" (Wickam, 2016) and "cowplot" packages (Wilke, 2020). Differences in water chemistry and physical conditions of the dams between seasons was evaluated using p-values from the Wilcoxon rank sum test applied to continuous variables and Fisher's exact test applied to categorical variables (trophic class).

We used two approaches to explore the drivers of GHGs in irrigation farm dams. First, individual linear mixed-effect models (LMEM) for CO_2, CH_4, and N_2O concentrations were developed to determine what environmental variables best explained the spatial variability in dissolved concentrations across dams. Independent variables tested included biotic (pH, DO, NH_4, NO_3, total dissolved N), abiotic (surface temperature, EC, area), management (dam type), and landscape factors (sediment C, N, C/N, soil pH, soil EC) that are known or presumed to influence aquatic GHG production. All potential model variables were checked for normality by visually inspecting histograms, transformed using either log, log10, square root, and checked again by performing a Shapiro-Wilk test ("shapiro.test" function). Before model fitting, variables were tested for collinearity by pair-wise linear regression to guide variable choice and avoid multicollinearity. First and second sampling campaign (spring or summer) was set as a fixed factor in the LMEM ("lmer" function in lme4 package, Bates et al. 2015) to account for repeated measures sampling design and dam identification set as a random factor. A combination of different variable types classified as biotic, abiotic, management, and landscape were individually tested in the LMEM until the best fit and most significant model was chosen. The models were evaluated through assessment of Q-Q plots, residuals versus predicted values, distribution of residual plots, and the final models were chosen based on the highest R^2 and lowest Akaike's information criterion.

To understand which irrigation farm dam types and conditions have the greatest impact on collective GHG emissions, we used individual LMEMs to determine whether season, size, farm dam type, and trophic status affected CO_2-equivalent (CO_2-eq) emissions. Dams were banded into four logarithmic bin classes (<0.001 km^2, 0.001-0.01 km^2, 0.01-0.1 km^2, and 0.1-1 km^2) that are commonly used to classify pond size classes (Holgerson et al. 2016). Trophic status was defined based on the total N concentration range for lakes in Smith et al (1999) and that used by the IPCC to adjust CH_4 EFs for lakes and reservoirs. Methane and N_2O were converted to CO_2-equivalent (CO_2-eq) emissions using the 100-year sustained-flux global warming potential (SGWP) and the sustained-flux global cooling potential (SGCP), where 1 kg of CH_4 is equivalent to 45 or 203 kg of CO_2 and 1 kg of N_2O is equivalent to 270 or 349 kg of CO_2 for emissions or uptake, respectively (Neubauer & Megonigal 2015). Total CO_2-eq emissions was estimated by taking the mean of each of the two samplings events and multiplying by the total days in spring and summer for each site. Data was log-transformed to fit a normal distribution. We added 130 units to total CO_2-eq emissions to avoid negative values during log transformation and set dam identification as a random factor. Models were evaluated as previously described with the other LMEMs and a 95% confidence interval was used to indicate significance.

Regional upscaling

To upscale total CO_2-eq emissions to the local irrigation region (MIA), we sourced the national farm dam map dataset (Malerba et al., 2020) and carried out the spatial analysis in R using the package "raster" (Hijmans, 2023). We adopted a similar approach to Audet et al. (2020) and estimated the density of irrigation dams by summing the number and total area of farm dams identified within a 10x10 km frame centred around Bilbul, an intensive irrigated cropping area consisting of winegrapes, rice, and broadacre crops in the MIA. A total of 124 dams were identified. The dams covered a total surface area of 35.3 ha, which yields a dam:irrigated landscape area ratio of 0.353%. Assuming the ratio is representative of all the region, irrigation dams would cover a total area of 13.38 km^2 in the MIA (378,911 ha, https://mirrigation.com.au, accessed 2 May 2023). Mean spring and summer CO_2-eq emissions were aggregated to obtain the total CO_2-eq emissions over the 6 month spring-summer irrigation season.

RESULTS

For most sites, the spring sampling period represented conditions of prolonged water storage prior to frequent irrigation and a cool-dry season. Both the 2021 and 2022 years experienced wetter than average conditions, recording annual rainfalls of 507.6 mm and 850.6 mm, respectively (Griffith, bom.gov.au).

Physical and environmental water conditions were highly variable between seasons. Mean water surface temperature was 10°C higher in summer (mean 25.6°C) and pH was also significantly higher (mean 8.93) compared with spring (mean 8.55, Table 1). Supersaturated oxygen conditions occurred in spring, with a mean DO of 135%, while oxygen conditions were near saturation in summer (mean 103%). Both the DO results and trophic status showed that most irrigation dams support high biological productivity, with 78% and 58% of dams either eutrophic or hypereutrophic in spring and summer, respectively. A lower proportion (10%) of settling ponds had eutrophic conditions during the study while 40% of recycle dams had eutrophic conditions at the time of sampling (Table S2). Phosphate and NO_3-N did not change significantly between the two surveys, although phosphate was below detection (<0.0025 mg L^{-1}) at 18 sites in spring compared to 8 sites in summer (Table 1).

Table 1: Summary of water quality variables, greenhouse gas concentrations, and trophic status across 38 farm dams during spring and summer. Presented as mean ± standard deviation (SD) for continuous

variables and count (percentage) for group variables.

Characteristic	Units	Spring, N = 37	Summer, N = 31	p-value[1]
Surface temperature	°C	15.5 (1.6)	25.6 (3.0)	<0.001
Dissolved oxygen	%	135 (30)	103 (41)	0.002
Electrical conductivity	$\mu S\ cm^{-1}$	326.4 (225.2)	419.4 (514.5)	0.845
pH		8.55 (0.73)	8.93 (0.75)	0.004
Phosphate	$mg\ P\ L^{-1}$	0.05 (0.04)	0.09 (0.11)	0.714
<0.025		18	8	
Ammonium	$mg\ N\ L^{-1}$	0.65 (0.50)	0.23 (0.17)	<0.001
Nitrate	$mg\ N\ L^{-1}$	0.72 (0.64)	1.10 (1.31)	0.662
CO_2	$\mu mol\ L^{-1}$	18.70 (24.50)	21.50 (29.57)	0.107
CH_4	$\mu mol\ L^{-1}$	2.20 (5.29)	1.35 (1.47)	0.893
N_2O	$nmol\ L^{-1}$	10.37 (6.57)	9.96 (11.90)	0.011
Trophic class				0.245[2]
Oligotrophic		2 (5.4%)	6 (19.4%)	
Mesotrophic		6 (16.2%)	7 (22.6%)	
Eutrophic		14 (37.8%)	8 (25.8 %)	
Hypereutrophic		15 (40.5%)	10 (32.2 %)	

[1]Wilcoxon rank sum test; [2]Fisher's exact test

Dissolved CO_2 and CH_4 concentrations did not vary between seasons (Table 1, *p* 0.107 and 0.893). Mean CO_2 was slightly higher than atmospheric equilibrium (11-15 $\mu mol\ L^{-1}$). Mean CH_4 was 2.20 $\mu mol\ L^{-1}$ and 1.35 $\mu mol\ L^{-1}$ in spring and summer, respectively, which is approximately 23-31 times greater than atmospheric equilibrium. Undersaturation between 0.02 $\mu mol\ L^{-1}$ and 0.07 $\mu mol\ L^{-1}$ was observed in seven sites in spring and two in summer, indicating an unusual occurrence of aquatic CH_4 uptake. Mean N_2O was higher in spring (10.37 nM) compared with summer (9.96 nM, p=0.011), following the same observation for NH_4^+ (Table 4, p<0.001).

Greenhouse gas drivers

The LMEM indicated that variation in CO_2 concentrations was best estimated by DO, NH_4^+, and sediment C content, with a significant difference between seasons and no dam size effect (Figure 1, Table S4 and S5). Overall, the model explained 54% of variance. Dissolved oxygen and NH_4^+ were the strongest predictors (p <0.001 and 0.004, respectively). Carbon dioxide displayed a positive association with increasing NH_4^+ (p=0.004) and sediment C (p=0.049), and lower concentrations with increasing DO (p<0.001) saturation.

Dissolved methane concentration was best explained by an interaction between soil salinity, trophic class, and size, while no seasonal effect was observed (Figure 2, Table S4 and S6). The LMEM explained 81% of CH_4 variance. Overall, CH_4 concentrations declined with increasing soil EC (p=0.036). The soil EC effect on CH_4 was strongest in oligotrophic dams which was different to eutrophic conditions where CH_4 instead did not decline with increasing soil EC (p=0.0321, Table S6). Small dams <0.001 km^2 had higher mean CH_4 concentrations (4.39 μmol L^{-1}) compared with those between 0.001 (p=0.0204, 1.12 μmol L^{-1}) ankm^2.1 km^2 (p=0.0287, 1.17 μmol L^{-1}) in surface area.

Nitrous oxide concentration was best explained by an interaction between DO and NH_4^+, and an interaction between size class and season (Figure 3, Table S4 and S6). The degree to which N_2O concentrations increased with NH_4^+ was influenced by DO saturation, where higher N_2O was observed when DO was low compared with supersaturated DO conditions (Figure 3A). The lowest N_2O concentrations occurred when both DO and NH_4^+ were low. The smallest dams (<0.001 km^2) had lower mean N_2O concentrations (8.82 nmol L^{-1}) than those between 0.001 (11.96 nmol L^{-1}, p=0.019) and 0.1 km^2 (9.29 nmol L^{-1}, p=0.005) and all dams had lower mean N_2O concentrations in summer (9.96 nmol L^{-1}, p=0.009). The difference between dam size was most pronounced in spring, when dams between 0.01–1 km^2 had higher N_2O than dams <0.001 km^2, whereas in summer no difference was detected between size classes (Figure 3B, Table S6).

Fluxes and CO_2-equivalent emissions

Approximately 48% of dams were emitters of CO_2, 87% were emitters of CH_4, and only 30% were emitters of N_2O (Figure S3) across both surveys (n=68). Estimated mean fluxes in spring (n=37) were 3.57 mmol m^{-2} d^{-1} (range: -13.28 to 63.7) for CO_2, 0.85 mmol m^{-2} d^{-1} (range: -0.02 to 12.5) for CH_4, and -0.33 μmol m^{-2} d^{-1} (range: -7.35 to 16.4) for N_2O. In summer (n=31), fluxes were 8.29 mmol m^{-2} d^{-1} (range: -3.99 to 101) for CO_2, 0.51 mmol m^{-2} d^{-1} (range: -0.01 to 2.75) for CH_4, and 1.26 μmol m^{-2} d^{-1} (range: -2.69 to 45.3) for N_2O.

Spring and summer had similar mean CO_2-eq emissions of 68 and 67 g CO_2-eq m^{-2} $season^{-1}$, respectively, although the contribution of CH_4 to CO_2-eq emissions were greater in spring (81%) compared to summer

(49%, Figure 4A). Smaller dams <0.001 km^2 had higher total CO_2-eq emissions (mean 305 g CO_2-eq m^{-2} $season^{-1}$, $p<0.05$) than larger ones (mean 46 and 111 g CO_2-eq m^{-2} $season^{-1}$ for 0.001-0.01 and 0.01-0.1 km^{-2}, respectively) except 0.1-1 km^2, where limited data was able to be collected. Settling ponds had lower net CO_2-eq emissions of 6.3 g CO_2-eq m^{-2} $season^{-1}$ over the entire summer irrigation season compared to recycle dams (249 g CO_2-eq m^{-2} $season^{-1}$, $p=0.040$). The GWP was highest in eutrophic waterbodies (174 g CO_2-eq m^{-2} $season^{-1}$) and lowest in mesotrophic waterbodies (45 g CO_2-eq m^{-2} $season^{-1}$) (Figure 4D). Overall, total CO_2-eq emissions from irrigation farm dams in the MIA are estimated to be 1,803 t CO_2-eq during the summer irrigation season.

DISCUSSION

Drivers of CO_2 and CH_4

Our spatial analysis of 38 irrigation farm dams revealed wide variations among CO_2 and CH_4 concentration. Approximately half of the irrigation farm dams were atmospheric CO_2 sinks at the time of sampling, with fluxes ranging from -13.3 to -0.20 mmol m^{-2} d^{-1} for uptake and 0.15 to 101 mmol m^{-2} d^{-1} for CO_2 sources. This proportion of farm dams acting as CO_2 sinks (52%) is identical to the 52% of farm dams (n = 100) found as CO_2 sinks in Saskatchewan (Jensen et al. 2023; Jensen et al. 2022; Webb et al. 2019b). On average CO_2 fluxes (mean 5.72 mmol m^{-2} d^{-1}) were lower than those reported in some Australian livestock dams (13.2-24.4 mmol m^{-2} d^{-1}) (Ollivier et al. 2019a; Ollivier et al. 2019b). Models showed that dam CO_2 concentrations were most strongly driven by internal metabolism (i.e., primary production and respiration) as DO saturation and NH_4^+ concentrations were the strongest predictors of CO_2 variance (Figure 1, Table S5). We interpret these patterns as relatively high inorganic N levels combined with direct sun exposure fueling autotrophic production and respiration beyond rates typical of natural ponds until excessive algal growth from N and warm temperatures promotes heterotrophic respiration at rates above autotrophic production (e.g., higher mean CO_2 in summer, Figure 2E and 4A). Farm dams tend to be highly productive freshwater ecosystems, and trends of O_2 production associated with CO_2 consumption are commonly observed (Webb et al., 2019b; Jensen et al. 2022; Malerba et al. 2022b). The particularly high mean DO conditions observed in irrigation dams may represent higher solar radiation exposure, lower organic carbon content of surrounding irrigated soils in the region (Webb et al. 2022) or limited organic matter inputs due to many dams being barren of vegetation (Table S1). The negative CO_2 association with DO also means that undertaking measurements during the day may underestimate the CO_2 flux estimates from these waterbodies due to the importance of both primary productivity and respiration in these dams. Limited studies have investigated diel CO_2 cycles in farm dams and have revealed contrasting findings, where waterbodies either remained as a CO_2 sink at night (Jensen et al., 2022) or remained a consistent source over diel cycles (Ollivier et al., 2019b).

Artificial waterbodies such as farm dams have recently become known as high emitters of CH_4, yet findings from this study revealed that most irrigation dams were relatively minor sources. Overall, 87% of irrigation dams were sources of CH_4 of the order 0.01 to 10.10 mmol m^{-2} d^{-1}, with some small negative to zero fluxes ranging from -0.02 to 0 mmol m^{-2} d^{-1}. The mean CH_4 emissions (diffusive flux) for irrigation dams of 0.69 mmol m^{-2} d^{-1} was 7-15 times lower than that of other farm dams in Victoria, NSW (diffusive), and Queensland (diffusive and ebullition) (Grinham et al. 2018; Ollivier et al. 2019a) and similar to temperate livestock dams in autumn and winter emissions (diffusive, 0.29-0.94 mmol m^{-2} d^{-1}) (Ollivier et al. 2019b; Malerba et al. 2022b).

Semi-arid irrigation dams in this study may support several environmental factors that minimise CH_4 production. First, most sites were oxygenated in the surface layer, with a mean DO of 120% across both surveys. Higher DO conditions are likely supressing anaerobic conditions and oxidising more CH_4 in the water column before being emitted to the atmosphere. The effect of higher oxygen conditions has been shown to reduce diffusive CH_4 emissions by 74% if increased from undersaturated to saturation oxygen conditions in livestock farm dams (Malerba et al. 2022b). The consistently high DO levels in the irrigation dams may also explain why no statistical association was found between CH_4 and DO.

Secondly, we found that dams <0.001 km^2 were higher in CH_4 emissions compared with those between 0.001-0.1 km^2 (Figures 2B and 4B). This finding reproduces a trend often observed in freshwater ponds and lakes, where higher CH_4 emissions occur due to small waterbodies supporting a higher sediment to water volume ratio and frequent water column mixing (Holgerson & Raymond 2016). However, most irrigation dams in the study area are larger than the average Australian farm dam area of 1000 m^2 (Malerba et al. 2021), with different dam types averaging 2,300 to 65,100 m^2, (Table S2). Even so, the smallest irrigation dams <0.001 km^2 still have lower average CH_4 concentrations (4.39 μmol L^{-1}) compared to the global pond average in this size group (7.57 μmol L^{-1}, Holgerson et al. 2016).

Characteristics of the surrounding soil and land use in the region may further contribute to lower CH_4 emissions compared with other farm dams in the country and global averages. Methane concentrations decreased in dams surrounded by soil with higher EC, which may mean there are more cations and anions into the waterbody, including sulphate which is known to suppress methanogenesis. This negative relationship of CH_4 with EC is typically observed for pond water conductivity (Pennock et al. 2010; Webb et al. 2019b), whereas here we found a direct relationship with surrounding soil properties. Another soil or land use effect may be that semi-arid soils are typically low in organic carbon and irrigation dams receive plant-based organic matter inputs rather than animal manure. These landscape controls such as mineral vs organic wetland, and the type of organic matter input, are well established factors that are included in the IPCC EF methodology for estimating CH_4 emissions from "Wetlands" and agricultural ponds under "Manure Management" (IPCC 2019).

Drivers of N_2O concentrations

Nitrous oxide exhibited a relatively narrow range of concentrations and was consistently low or undersaturated (Table 1). Nitrous oxide uptake ranged from -7.35 to -0.09 μmol m^{-2} d^{-1} and emissions from 0.01 to 45.3 μmol m^{-2} d^{-1} (Figure S3). Nitrous oxide consumption across the majority of irrigation dams suggests that complete denitrification dominates over N_2O production, and that this was strongest at low DO and NH_4^+ levels (Figure 3A). Although N loading is assumed to drive global riverine and lake N_2O production (Lauerwald et al. 2019; Yao et al. 2020), here we did not find a straightforward relationship between surface water N availability and N_2O. Instead, there was no relationship with NO_3^-, and the N_2O with NH_4^+ relationship was dependent on DO. Studies on lakes and artificial aquatic ecosystems have shown an association between N_2O consumption and primary production (Borges et al. 2022; Ferrón et al. 2012; Jensen et al. 2023; Webb et al. 2019a). Our study adds further evidence that variation in N_2O is not proportional to changes in surface water inorganic N levels and is controlled partly by oxygen levels and/or autotrophy. The reasons are not entirely known and may be attributed to primary producer competition for N substrates (Webb et al. 2019a) in productive waters which leads to a stoichiometric N deficit (Scott et al. 2019), oxygen stratification controlling the penetration of inorganic N with depth (Christensen et al. 1990; Rysgaard et al. 1994), supply of organic matter to sediments, or microalgae assimilation (Ferrón et al. 2012). Further evidence that primary productivity controls N_2O is revealed by the size class relationship found between irrigation dams, where differences between dam size was only observed during spring and not summer (Figure 3B). Regardless, these factors explain less than half of N_2O variability, indicating that other environmental factors not measured are at play.

Approximately 70% of irrigation farm dams were N_2O sinks, representing the first known study in the Southern Hemisphere to demonstrate such widespread N_2O uptake in agricultural waters. A study of GHGs from 100 semi-arid farm dams in Canada found 67% of these waterbodies behaving as N_2O sinks (Webb et al., 2019a): something that had only previously been observed in natural, low-nitrogen, fresh waterbodies (Soued et al. 2015). Analysis of the literature has revealed that the current IPCC methodology often overestimates N_2O emissions from artificial agricultural waters, especially ponds (Tian et al. 2019; Webb et al. 2021). Using the ratio of N_2O-N to NO_3-N concentrations, the mean EF from this study was 0.06% (range: 0.003-0.41%); substantially lower than the IPCC EF_5 of 0.26% (CI: 0.16-0.36) for indirect surface water emissions. Semi-arid agricultural soils also emit significantly less fertiliser-derived N_2O than the global average, suggesting there may be a climate-zone soil effect (Barton et al. 2008). The effect of diel cycles on N_2O needs to be considered in future refinement of EFs as most N_2O measurements from artificial and natural ponds are taken during sunlight hours when primary production (and thus surface water O_2 concentration) is at its peak. It is unclear whether this sampling bias would lead to an under or overestimation of pond N_2O emissions as we observed N_2O sinks at both low and high dissolved oxygen conditions. Inconsistent relationships between diel fluctuations in surface water O_2 and N_2O are also reported across the freshwater literature (Baulch et al. 2011; Jensen et al. 2022; Wells & Eyre 2021), likely because lower O_2 can either enhance N_2O production or increase its reduction to N_2. Ultimately, this study challenges traditional understanding that high N loads lead to proportionally high N_2O emissions in freshwaters and begs for further research on how different types of artificial waters function in terms of N_2O production and consumption.

Management opportunities

Our study on semi-arid irrigation farm dams reinforces findings that managing nutrient enrichment is key to curbing total CO_2-eq emissions in farm dams (Malerba et al. 2022b; Webb et al. 2019b). Evidence from the LMEMs show that reducing nutrients, particularly inorganic N, may diminish both CH_4 (Figure 2), N_2O (Figure 3), and overall CO_2-eq emissions (Figure 4D). While not significant, the trophic status of the dam had a distinct impact on total CO_2-equivalent emissions. If irrigation farm dams were managed to avoid eutrophication, this could represent a CO_2-eq emissions saving of 0.35-1.29 t CO_2-eq ha^{-1} over the summer irrigation season (180 days). This is consistent with the 0.81 t CO_2-eq ha^{-1} emissions from CH_4 estimated to be avoided if livestock farm dams were fenced to reduce nutrients (Malerba et al. 2022b).

Even greater emission savings of 2.05-2.62 t CO_{2}-eq ha^{-1} could be achieved if new dams were 0.1-10 ha^{-1} instead of <0.1 ha in size (Figure 4B). Small waterbodies will concentrate nutrient inputs and have greater contact with organic matter-rich sediment, which can make them hotspots for carbon emissions (Holgerson 2015), although not necessarily N_2O emissions (Figure 3B, Borges et al. 2022; Webb et al. 2019a). Creating deeper dams may be an option to simultaneously dilute fertiliser runoff, reduce eutrophication with cooler waters, and allow for conditions that promote CH_4 oxidation in the epilimnion (Borges et al. 2022; Webb et al. 2019b).

Sediment settling ponds on horticultural farms may hold clues for GHG management in other types of irrigation farm dams. Of all dam types in this study, settling ponds had the lowest net CO_2-eq emissions due to CO_2 and N_2O uptake offsetting most of the diffusive CH_4 emissions. Recycle dams, however, were found to have a higher GWP of 249 g CO_2-eq m^{-2} $season^{-1}$. This may be due to differences in water management, including a shorter water residence time, more frequent wet-dry cycles in recycle dams, and more soil and fertiliser N runoff from surface furrow irrigation for recycle dam types compared to drip irrigation used specifically in horticultural systems. Settling ponds accumulate sediment and improve water quality due to the need to reduce emitter clogging in drip irrigation infrastructure (Bonachela et al. 2013). Therefore, the low flows and permanently flooded conditions likely allows for more removal of reactive N (Tournebize et al. 2015). Here, this can be demonstrated by lower NH_4^+ and NO_3^- in settling ponds compared with recycle dams (p=0.006 and 0.04) with an overall greater proportion of recycle dams in a eutrophic state (Table S2).

Managing the amount of nutrients in recycle dams is difficult as irrigation water comes into direct contact with soil and fertiliser. However, in-field practices to retain nutrients or reduce fertiliser application would translate into less nutrients flowing into the dam, presenting a win-win for managing field and water farm emissions and crop nutrient use efficiency. Floating wetlands have been shown to reduce methane production in wetland environments that are known high CH_4 producers and may be worth trialling in recycle dams as an option (Wang et al. 2024). Alternatively, having strips of vegetation in drainage channels may be an effective and simple treatment option for removing fertiliser N runoff before entering the dam (Zhang et al. 2016).

Implications of emission estimates when compared with the available data

Our synoptic GHG survey of irrigation farm dams during the summer irrigation season demonstrates that emissions are substantially lower than other farm dams and artificial ponds (Table 2). This study is the first to report all three GHGs from irrigation farm dams and found that CO_2-eq emissions were 2.8-21 times lower compared with artificial ponds and 2.9-9.1 times lower compared with most farm dams/reservoirs. Semi-arid irrigation farm dams had mean spring-summer CO_2-eq emissions of 0.76 ± 2.20 g CO_2-eq m^{-2} d^{-1}, which were within the range of temperate farm dams in winter (0.83 g CO_2-eq m^{-2} d^{-1}) and some shrimp and fish aquaculture ponds (0.41 g CO_2-eq m^{-2} d^{-1}). Carbon dioxide emissions in semi-arid dams were lower than those measured in other regions using one-off spot sampling during similar times of the day. Although daily CO_2 emissions rates are likely underestimated by our 'daytime' sampling approach due to the strong autotrophic control on CO_2 accumulation in the studied farm dams (Figure 1A), this does not explain the regional differences suggested by our study. This indicates that some spatial nuances are likely occurring. Given well documented variability in the magnitude of diurnal CO_2 fluctuations (i.e., the ratio of productivity to respiration) in ponds (Brothers & Vadeboncoeur 2021), future work integrating GHG emissions over diel cycles is needed to precisely determine the magnitude of these spatial differences.

This is the second reported study to observe such a high proportion of CO_2 (52%) and N_2O (70%) sinks in small artificial waterbodies across an agricultural region (Webb et al., 2019a, b) and the first reported in the Southern Hemisphere. On average, our study had even lower CO_2, CH_4, and N_2O emissions compared with the semi-arid farm dams in Canada where widespread CO_2 and N_2O sinks in farm dams (livestock and cropping) were originally observed (Table 2). Although both regions are classified as semi-arid in terms of their annual precipitation, they have largely different seasonality. Only two other studies are known to have directly measured GHGs from irrigation farm dams (Table 2). Compared with subtropical irrigation ponds, CH_4 emissions were 8-times lower (Grinham et al., 2018) and similar for N_2O (Macdonald et al., 2016). These comparisons beg the question, are climate or regional factors driving these differences and how this may impact emission estimates at continental to global scales?

Table 2: Comparison of mean CO_2, CH_4, N_2O and total CO_2-equivalent emissions from farm dams and artificial ponds from the literature. All CO_2-equivalent fluxes were calculated using the 100-yr sustained global warming potential (1g CH_4 = 45 g CO_2, 1 g N_2O = 270 g CO_2) or sustained global consumption potential (1 g CH_4 = 203 g CO_2, 1 g N_2O = 349 g CO_2) from Neubauer and Megonigal (2015).

Waterbody	CO_2 (mmol m^{-2} d^{-1})	CH_4 (mmol m^{-2} d^{-1})	N_2O (μmol m^{-2} d^{-1})	CO_2-eq (g CO_2 m^{-2} d^{-1})	Reference
Temperate farm dams – summer, Australia	24.4 ± 3.56	7.2 ± 1.74		6.26 ± 1.41	Ollivier et al. (2018)
Temperate farm dams – winter, Australia	13.2 ± 2.96	0.29 ± 0.04	3.05 ± 0.68	0.83 ± 0.17	Ollivier et al. (2019)
Subtropical stock farm dams, Australia		10.5			Grinham et al. (2018)
Subtropical irrigation farm dams		5.25			Grinham et al. (2018)
Agricultural and urban ponds, India	67.1 ± 64	17.9 ± 18.5		15.84 ± 16.14	Panneer et al. (2014)
Subtropical aquaculture ponds, China	-33.0–11.3	2.48–29.9	5.86–6.44	0.41–22.1	Yang et al., 2015
Urban ponds, Sweden	17.1 (-4.25–78.4)	1.89 (0.02–10.8)		2.12 ± 0.43	Peacock et al. (2019)
Urban ponds, Denmark	52.3 ± 66.3	1.25 ± 5.83	6.79 ± 22.5	3.28 ± 7.38	Audet et al. (2020)
Semi-arid agricultural reservoirs – summer, Canada	41.3 ± 94.9	7.11 ± 12.0	1.46 ± 19.9	6.95 ± 13.1	Webb et al. (2019a, b)
Semi-arid agricultural reservoirs – seasonal, Canada	19.7 ± 56.6	2.90 ± 10.9	9.70 ± 52.9	3.02 ± 10.7	Jensen et al. (2022)
Temperate livestock dams, Australia	33.9 (-38.6–318)	0.94 (0.01–10.2)		2.17	Malerba et al. (2022b)
Global EF for freshwater constructed waterbodies (CH_4) and agricultural surface waters (N_2O)[a]		3.13 (CI: 2.02–3.89)	57.5 (CI: 33.0–82.0)	2.94 (1.85–3.77)	IPCC (2019)
Subtropical irrigation storage, Australia			0.24-1.24		Macdonald et al. (2016)[b]
Semi-arid irrigation farm dams, Australia	5.72 (-13.3–101)	0.69 (-0.02–12.5)	0.39 (-7.35–45.3)	0.76 ± 2.20	This study

[a]The IPCC N_2O flux shown here was calculated for our study by applying the 0.26% EF_5 for rivers and lakes to our study mean NO_3^- concentration (0.9 mg N L^{-1}), then using the resulting N_2O concentration to calculate the flux using our farm dam-specific k_{600} value of 0.76. Confidence interval (CI) was used to show range in estimate for IPCC emission factors instead of standard deviation which is more commonly reported in individual studies.

[b]Based on total seasonal emissions estimated from both floating chamber and dissolved N_2O derived flux

Using the IPCC EF estimates for "*freshwater constructed waterbodies*" and *"agricultural surface waters"* would vastly overestimate emissions from semi-arid irrigation farm dams in this region. Applying the study average EF of 40 kg CH_4 ha^{-1} yr^{-1} and N_2O flux of 0.39 µmol m^{-2} d^{-1} would yield regional scale emissions of 27 t CH_4 $season^{-1}$ and 0.06 t N_2O $season^{-1}$ from irrigation dams. If we exclude all negative fluxes measured from the study, as the IPCC EF model assumes that artificial waterbodies only emit CH_4 and N_2O, regional irrigation dam emissions would be 31 t CH_4 $season^{-1}$ and 0.7 t N_2O $season^{-1}$. This compares with 122 t CH_4 $season^{-1}$ and 4.5 t N_2O $season^{-1}$ when using the current best EF estimates of 183 kg CH_4 ha^{-1} yr^{-1} and applying the 0.26% N_2O-N:NO_3-N ratio available from the IPCC (2019) to our mean NO_3^- concentration (0.90 mg N L^{-1}). This provides a first order estimate on the potential level of overestimation if semi-arid irrigation dams were assumed to emit the same level of CH_4 and N_2O emissions as the global standard for small artificial freshwaters and agricultural surface waters.

CONCLUSION

In a world first, we assessed CO_2, CH_4, and N_2O emissions from semi-arid irrigation farm dams. This dataset will help refine global EF estimates and Australia's farm dam contribution to the national GHG inventory. We show that these waterbodies are minor sources of GHGs relative to previous studies, despite them being nutrient enriched farm waterbodies, which brings a new perspective to our understanding that not all artificial or nitrogen-polluted waterbodies are large CH_4 and N_2O emitters. The exact reason for this remains to be investigated but may be due to a combination of a semi-arid climate providing high sunlight exposure, regional soil and land use factors, and irrigation dam management. Although CH_4 emissions were comparatively low for farm dams, CH_4 still contributed the highest CO_2-eq emissions and often offset any CO_2 or N_2O uptake measured at the time of sampling Therefore, developing strategies for mitigating CH_4 emissions in irrigation dams would deliver the greatest results on reducing the farm dam carbon footprint. Most importantly, we show that the magnitude of emissions from artificial waterbodies in the studied irrigated catchment would be vastly overestimated using global averages. As no diel factors were found to drive dam CH_4, we propose that spatial coverage, rather than diel fluctuations, are the focus of future efforts to constrain CH_4 emissions factors from agricultural waterbodies. Therefore, to refine GHG emission estimates for agricultural and artificial waterbodies, we urge further research across two areas: 1) perform measurements in other irrigation areas from other climatic regions to assess whether the markedly lower CH_4 and N_2O emissions observed here are a product of irrigation dams themselves or climate or geographical features, and 2) integrate diel cycles into GHG measurements to reduce bias in under or overestimating CO_2 and N_2O.

Declarations

Funding

This work was funded by AgriFutures Australia and Deakin University (project PRO-015008). JRW would like to acknowledge Deakin University for seed funding through the Peer-Review, ECR Support and the Mini ARC Analog Programme – Linkage schemes to enable pilot data collection and equipment purchase.

Acknowledgements

We extend our thanks to the farmers who participated in this study by generously allowing our research team onto their farms to sample dams and the knowledge they imparted. To Julian Hill for guiding project management with AgriFutures Australia. A special mention to students Samantha Taylor and Lucas D'Monte, who helped with field work tasks. The Irrigation Research and Extension Committee (Iva Qarisa, IREC) and Rice Research Australia (Neil Bull) for dam access (Whitton and RRAPL) and connecting us with growers.

Competing Interests

The authors declare no conflict of interest.

Data availability

The data generated in this study are freely available on GitHub (https://github.com/JackieRWebb/Irrigation-dams-GHGs).

References

1. Aguilera E, Vila-Traver J, Deemer BR, Infante-Amate J, Guzmán GI, González de Molina M (2019). Methane Emissions from Artificial Waterbodies Dominate the Carbon Footprint of Irrigation: A Study of Transitions in the Food–Energy–Water–Climate Nexus (Spain, 1900–2014). Environmental Science & Technology:
2. Australian Bureau of Meteorology (2023). Monthly climate statistics, Griffith Airport (01-01-2003 to 01-01-2023). Downloaded from http://www.bom.gov.au/ on 01-07-2023

3. Barton L, Kiese R, Gatter D, Butterbach-Bahl K, Buck R, Hinz C, Murphy DV (2008) Nitrous oxide emissions from a cropped soil in a semi-arid climate. Global Change Biology 14(1): 177-192
4. Baulch HM, Dillon PJ, Maranger R, Venkiteswaran JJ, Wilson HF, Schiff SL (2012) Night and day: short-term variation in nitrogen chemistry and nitrous oxide emissions from streams. Freshwater Biology 57(3): 509-525
5. Bonachela S, Juan M, Casas JJ, Fuentes-Rodríguez F, Gallego I, Elorrieta MA (2013). Pond management and water quality for drip irrigation in Mediterranean intensive horticultural systems. Irrigation Science 31(4): 769-780
6. Borges AV, Deirmendjian L, Bouillon S, Okello W, Lambert T, Roland FAE, Razanamahandry VF, Voarintsoa NRG, Darchambeau F, Kimirei IA, Descy J-P, Allen GH, Morana C (2022). Greenhouse gas emissions from African lakes are no longer a blind spot. Science Advances 8(25): eabi8716
7. Brothers, S. and Vadeboncoeur, Y. (2021) Shoring up the foundations of production to respiration ratios in lakes. Limnol. Oceanogr. 66, 2762-2778.
8. Christensen PB, Nielsen LP, Sørensen J, Revsbech NP (1990). Denitrification in nitrate-rich streams: Diurnal and seasonal variation related to benthic oxygen metabolism. Limnology and Oceanography 35(3): 640-651
9. Craig, I., Green, A., Scobie, M. & Schmidt, E (2005). Controlling Evaporation Loss from Water Storages Publication No 1000580/1 (National Centre for Engineering in Agriculture).
10. Douglas Bates, Martin Maechler, Ben Bolker, Steve Walker (2015). Fitting Linear Mixed-Effects Models Using lme4. Journal of Statistical Software, 67(1), 1-48. doi:10.18637/jss.v067.i01.
11. Ferrón S, Ho DT, Johnson ZI, Huntley ME (2012) Air–Water Fluxes of N_2O and CH_4 during Microalgae (Staurosira sp.) Cultivation in an Open Raceway Pond. Environmental Science & Technology 46(19): 10842-10848
12. Grinham A, Albert S, Deering N, Dunbabin M, Bastviken D, Sherman B, Lovelock CE, Evans CD (2018). The importance of small artificial water bodies as sources of methane emissions in Queensland, Australia. Hydrol. Earth Syst. Sci. 22(10): 5281-5298
13. Hijmans R (2023) raster: Geographic Data Analysis and Modeling. R package version 3.6-14, https://CRAN.R-project.org/package=raster.
14. Holgerson MA (2015). Drivers of carbon dioxide and methane supersaturation in small, temporary ponds. Biogeochemistry 124(1): 305-318
15. Holgerson MA, Raymond PA (2016) Large contribution to inland water CO_2 and CH_4 emissions from very small ponds. Nature Geoscience 9: 222
16. Hope D, Palmer SM, Billett MF, Dawson JJC (2004). Variations in dissolved CO_2 and CH_4 in a first-order stream and catchment: an investigation of soil–stream linkages. Hydrological Processes 18(17): 3255-3275
17. IPCC (2019). 2019 Refinement to the 2006 IPCC Guidelines for National Greenhouse Gas Inventories.

18. Jensen SA, Webb JR, Simpson GL, Baulch HM, Leavitt PR, Finlay K (2022). Seasonal variability of CO_2, CH_4, and N_2O content and fluxes in small agricultural reservoirs of the northern Great Plains. Frontiers in Environmental Science 10:
19. Jensen SA, Webb JR, Simpson GL, Baulch HM, Leavitt PR, Finlay K (2023). Differential Controls of Greenhouse Gas (CO_2, CH_4, and N_2O) Concentrations in Natural and Constructed Agricultural Waterbodies on the Northern Great Plains. Journal of Geophysical Research: Biogeosciences 128(4): e2022JG007261
20. Lauerwald R, Regnier P, Figueiredo V, Enrich-Prast A, Bastviken D, Lehner B, Maavara T, Raymond P (2019). Natural Lakes Are a Minor Global Source of N_2O to the Atmosphere. Global Biogeochemical Cycles 33(12): 1564-1581
21. Lindroth, A., Tranvik, L (2021). Accounting for all territorial emissions and sinks is important for development of climate mitigation policies. Carbon Balance Manage 16, 10. https://doi.org/10.1186/s13021-021-00173-8
22. Macdonald BCT, Nadelko A, Chang Y, Glover M, Warneke S (2016). Contribution of the cotton irrigation network to farm nitrous oxide emissions. Soil Research 54(5): 651-658
23. Malerba ME, de Kluyver T, Wright N, Schuster L, Macreadie PI (2022a). Methane emissions from agricultural ponds are underestimated in national greenhouse gas inventories. Communications Earth & Environment 3(1): 306
24. Malerba ME, Lindenmayer DB, Scheele BC, Waryszak P, Yilmaz IN, Schuster L, Macreadie PI (2022b). Fencing farm dams to exclude livestock halves methane emissions and improves water quality. Global Change Biology 28(15): 4701-4712
25. Malerba ME, Wright N, Macreadie PI (2021). A Continental-Scale Assessment of Density, Size, Distribution and Historical Trends of Farm Dams Using Deep Learning Convolutional Neural Networks. Remote Sensing 13(2): 319
26. McDermid S, Nocco M, Lawston-Parker P, Keune J, Pokhrel Y, Jain M, Jägermeyr J, Brocca L, Massari C, Jones AD, Vahmani P, Thiery W, Yao Y, Bell A, Chen L, Dorigo W, Hanasaki N, Jasechko S, Lo M-H, Mahmood R, Mishra V, Mueller ND, Niyogi D, Rabin SS, Sloat L, Wada Y, Zappa L, Chen F, Cook BI, Kim H, Lombardozzi D, Polcher J, Ryu D, Santanello J, Satoh Y, Seneviratne S, Singh D, Yokohata T (2023) Irrigation in the Earth system. Nature Reviews Earth & Environment:
27. National Farmers Federation (2020). 2030 Roadmap: Australian Agriculture's Plan for a $100 Billion Dollar Industry, https://nff.org.au/wp-content/uploads/2020/02/NFF_Roadmap_2030_FINAL.pdf
28. Neubauer SC, Megonigal JP (2015). Moving Beyond Global Warming Potentials to Quantify the Climatic Role of Ecosystems. Ecosystems: 1-14
29. Ollivier QR, Maher DT, Pitfield C, Macreadie PI (2019a). Punching above their weight: Large release of greenhouse gases from small agricultural dams. Global Change Biology 25(2): 721-732
30. Ollivier QR, Maher DT, Pitfield C, Macreadie PI (2019b). Winter emissions of CO_2, CH_4, and N_2O from temperate agricultural dams: fluxes, sources, and processes. Ecosphere 10(11): e02914

31. Panneer Selvam B, Natchimuthu S, Arunachalam L, Bastviken D (2014) Methane and carbon dioxide emissions from inland waters in India – implications for large scale greenhouse gas balances. Global Change Biology 20(11): 3397-3407
32. Peacock M, Audet J, Bastviken D, Cook S, Evans CD, Grinham A, Holgerson MA, Högbom L, Pickard AE, Zieliński P, Futter MN (2021). Small artificial waterbodies are widespread and persistent emitters of methane and carbon dioxide. Global Change Biology 27(20): 5109-5123
33. Peacock M, Audet J, Jordan S, Smeds J, Wallin MB (2019). Greenhouse gas emissions from urban ponds are driven by nutrient status and hydrology. Ecosphere 10(3): e02643
34. Pennock D, Yates T, Bedard-Haughn A, Phipps K, Farrell R, McDougal R (2010). Landscape controls on N_2O and CH_4 emissions from freshwater mineral soil wetlands of the Canadian Prairie Pothole region. Geoderma 155(3): 308-319
35. R Core Development Team (2022). A language and environment for statistical computing. R Foundation for Statistical Computing, Vienna, Austria
36. Rysgaard S, Risgaard-Petersen N, Niels Peter S, Kim J, Lars Peter N (1994). Oxygen regulation of nitrification and denitrification in sediments. Limnology and Oceanography 39(7): 1643-1652
37. Scott JT, McCarthy MJ, Paerl HW (2019). Nitrogen transformations differentially affect nutrient-limited primary production in lakes of varying trophic state. Limnology and Oceanography Letters 4(4): 96-104
38. Smith VH, Tilman GD, Nekola JC (1999). Eutrophication: impacts of excess nutrient inputs on freshwater, marine, and terrestrial ecosystems. Environmental Pollution 100 (1): 179-196
39. Soued C, del Giorgio PA, Maranger R (2015). Nitrous oxide sinks and emissions in boreal aquatic networks in Québec. Nature Geoscience 9: 116
40. Tian L, Cai Y, Akiyama H (2019). A review of indirect N_2O emission factors from agricultural nitrogen leaching and runoff to update of the default IPCC values. Environmental Pollution 245: 300-306
41. Tournebize J, Chaumont C, Fesneau C, Guenne A, Vincent B, Garnier J, Mander Ü (2015). Long-term nitrate removal in a buffering pond-reservoir system receiving water from an agricultural drained catchment. Ecological Engineering 80: 32-45
42. United Nations Framework Convention on Climate Change (2022). National Inventory Submissions 2021. https://unfccc.int/ghg-inventories-annex-iparties/2021.
43. Wang F, Zhang S, Hu X, Lv X, Liu M, Ma Y, Manirakiza B (2024). Floating plants reduced methane fluxes from wetlands by creating a habitat conducive to methane oxidation. Journal of Environmental Sciences 135: 149-160
44. Webb, J. R., Awale, R., & Quayle, W. (2022). Spatial patterns of CO2 fluxes across litter amended, non-amended, and native soils on cotton farms in southern NSW. In Proceedings of the 20th Australian agronomy conference, Toowoomba, Qld, Australia.
45. Webb JR, Clough TJ, Quayle WC (2021). A review of indirect N_2O emission factors from artificial agricultural waters. Environmental Research Letters 16(4): 043005

46. Webb JR, Hayes NM, Simpson GL, Leavitt PR, Baulch HM, Finlay K (2019a). Widespread nitrous oxide undersaturation in farm waterbodies creates an unexpected greenhouse gas sink. Proceedings of the National Academy of Sciences: 201820389
47. Webb JR, Leavitt PR, Simpson GL, Baulch HM, Haig HA, Hodder KR, Finlay K (2019b). Regulation of carbon dioxide and methane in small agricultural reservoirs: optimizing potential for greenhouse gas uptake. Biogeosciences 16(21): 4211-4227
48. Wells, N.S. and Eyre, B.D. (2021) Flow regulates biological NO_3- and N_2O production in a turbid sub-tropical stream. Geochim. Cosmochim. Acta 306, 124-142
49. H. Wickham. ggplot2: Elegant Graphics for Data Analysis. Springer-Verlag New York, 2016.
50. Wilke C (2020). _cowplot: Streamlined Plot Theme and Plot Annotations for 'ggplot2'_. R package version 1.1.1, https://CRAN.R-project.org/package=cowplot.
51. Weiss RF (1974). Carbon dioxide in water and seawater: the solubility of a non-ideal gas. Marine Chemistry 2(3): 203-215
52. Weiss RF, Price BA (1980). Nitrous oxide solubility in water and seawater. Marine Chemistry 8(4): 347-359
53. Yamamoto S, Alcauskas JB, Crozier TE (1976). Solubility of methane in distilled water and seawater. Journal of Chemical and Engineering Data 21(1): 78-80
54. Yang P, He Q, Huang J, Tong C (2015). Fluxes of greenhouse gases at two different aquaculture ponds in the coastal zone of southeastern China. Atmospheric Environment 115(Supplement C): 269-277
55. Yao Y, Tian H, Shi H, Pan S, Xu R, Pan N, Canadell JG (2020). Increased global nitrous oxide emissions from streams and rivers in the Anthropocene. Nature Climate Change 10(2): 138-142
56. Zhang S, Liu F, Xiao R, Li Y, He Y, Wu J (2016). Effects of vegetation on ammonium removal and nitrous oxide emissions from pilot-scale drainage ditches. Aquatic Botany 130: 37-44

Figures

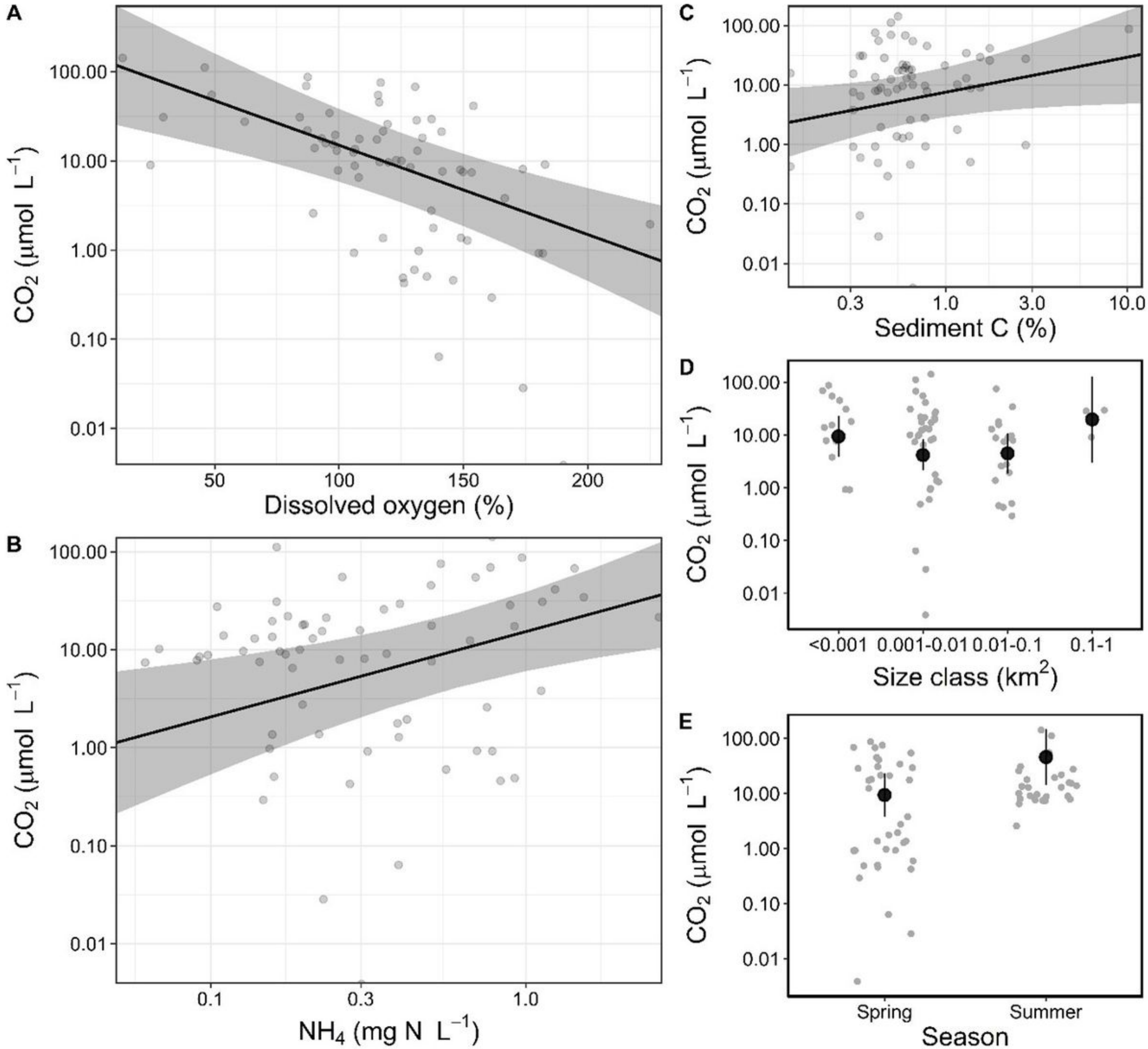

Figure 1

Partial effects plots from the linear mixed effect model illustrating the response of surface water CO_2 concentrations with: A) dissolved oxygen saturation (%); B) ammonium (mg N L^{-1}); C) sediment carbon content (%); D) dam size classificatiokm^{2}km^2); and E) season. Shaded area in A, B, and C indicates 95% credible intervals, while grey circles are the raw observed data. The conditional R^2 was 0.54.

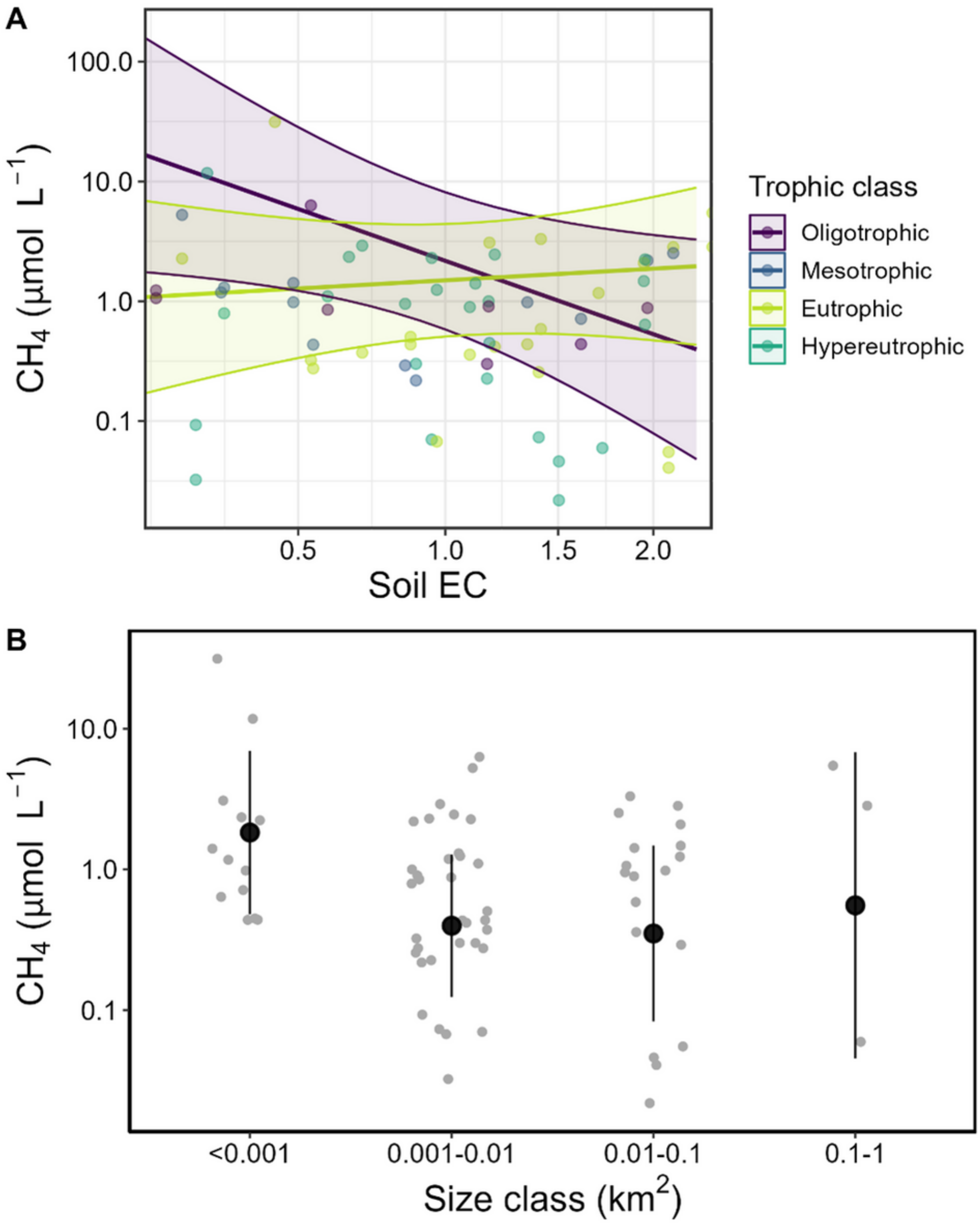

Figure 2

Partial effects plots from the linear mixed effect model illustrating the response of surface water CH_4 concentrations with: A) an interaction between soil electrical conductivity (mS cm^{-1}) and trophic class: and B) dam size classifkm^2tion (km^2). Shaded area in A indicates 95% credible intervals, while circles are the raw observed data. Error bars in B represent confidence intervals from the LMEM. Only responses that were significantly different from each other are shown with regression line in *A*. The conditional R^2 was 0.81.

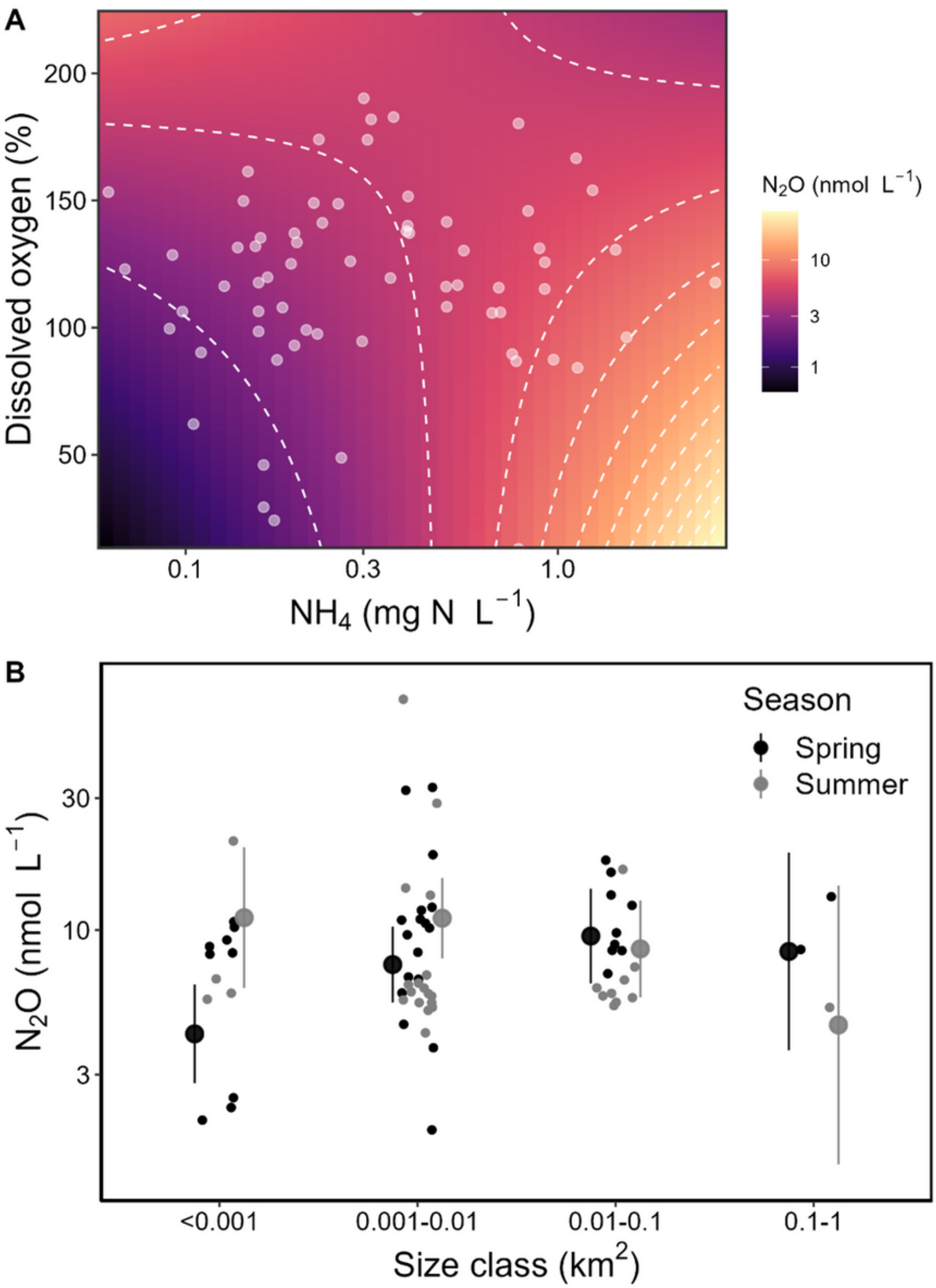

Figure 3

Partial effects plots from the linear mixed effect model illustrating the response of surface water N_2O concentrations with: A) an interaction between surface water NH_4^+ concentrations and dissolved oxygen saturation: and B) an interaction between dam size classification (km^2) and season where error bars represent confidence intervals from the LMEM. White circles are the raw observed data. The conditional R^2 was 0.44.

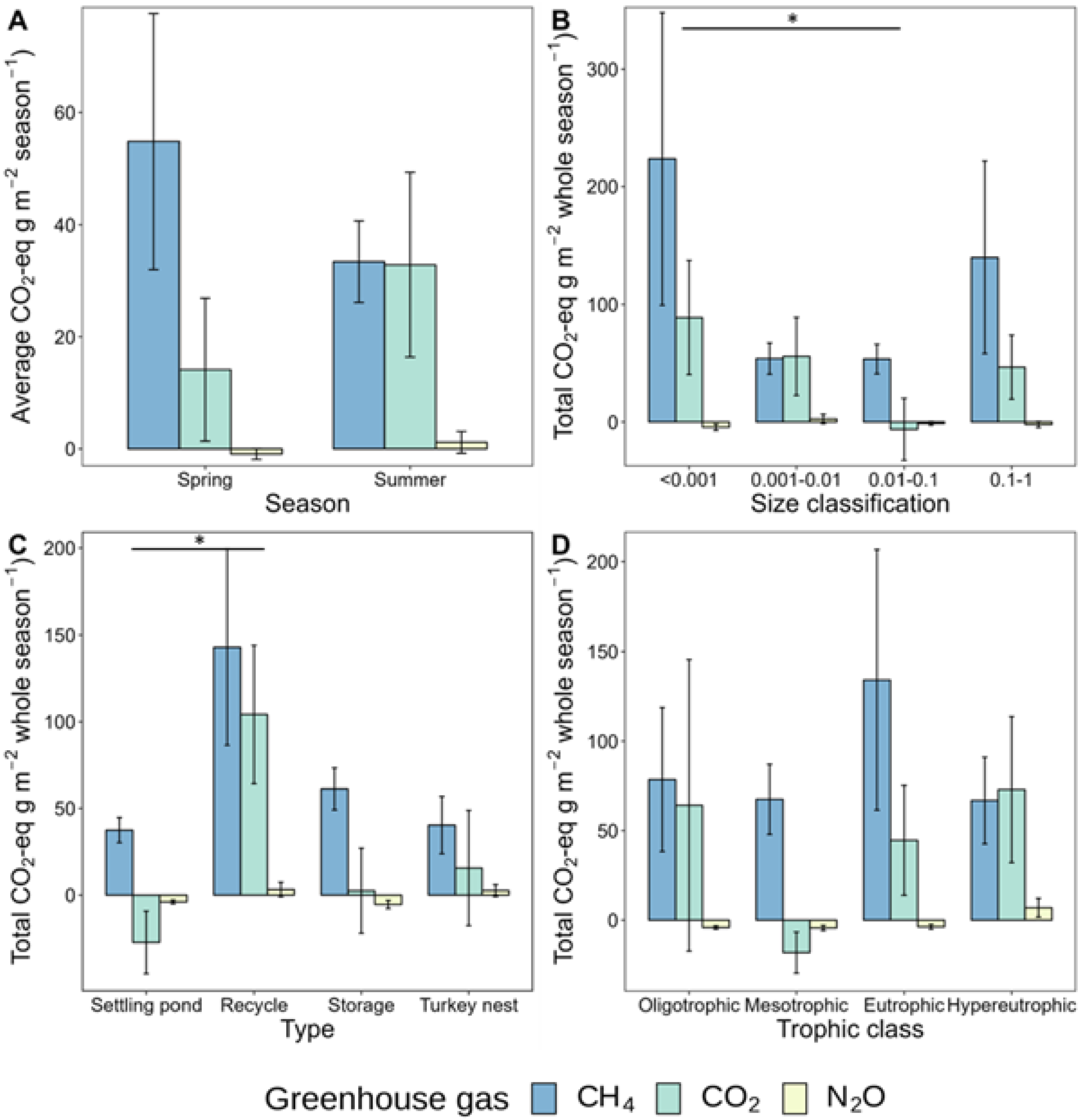

Figure 4

CO_2-equivalent fluxes from on-farm irrigation dams for each season (A) and over the whole irrigation season (180 days) in the MIA and CIA by waterbody size classification (B), waterbody type (C), and trophic classification (D). Linear mixed-effect models indicated significant differences in total CO_2-equivalent emissions between dams <0.001 ha and 0.001-0.1 ha in size, and between settling ponds and recycle dams (p <0.05).

Supplementary Files

This is a list of supplementary files associated with this preprint. Click to download.

- Supplementaryinformation.docx